PORT SAID ENGINEERING RESEARCH JOURNAL

Faculty of Engineering - Port Said University
Volume (28) No. 3 pp: 132:139

Distortion Analysis of Steel Stiffened Plates Accounting for Different Welding Configurations

S. Saad-Eldeen[1], M-Allah Eltaramsy[2], M. Mansour, [3]*

[1] *Naval Architecture and Marine Engineering Department, Faculty of Engineering, Port Said University, Port Said, Egypt, saad.bahey@eng.psu.edu.eg*

[2] *Naval Architecture and Marine Engineering Department, Faculty of Engineering, Port Said University, Port Said, Egypt, mena.elsayed@eng.psu.edu.eg*

[3] *Naval Architecture and Marine Engineering Department, Faculty of Engineering, Port Said University, Port Said, Egypt, sohimo@hotmail.com*

**Corresponding author, DOI: 10.21608/PSERJ.2024.251565.1294*

Received 6-12-2023
Revised 11-3-2024
Accepted 13-3-2024

ABSTRACT

The present work presents a series of experimental distortion analysis of square shipbuilding steel plates with an attached stiffener. Two approved fillet welding configurations are applied to attach the stiffener using shielded metal arc welding at Port Said Shipyard. The specimens are welded using continuous and intermittent chain fillet welding for variant plating thicknesses with constant stiffener geometrical configurations, where two welding passes are applied. The effect of different fillet welding geometry on the induced initial imperfection amplitudes for different base plating thicknesses is investigated. The imperfection shapes are tracked, and the amplitudes are measured during and after the welding process. The imperfection amplitudes for each plating thickness and welding geometry are analyzed considering both preheat after the first pass and heat relief. Several relationships considering the welding time and the amount consumed electrodes are performed for different plating thicknesses and welding geometries. A comparison between existing empirical formulations and the observed results is performed in the form of plate slenderness, showing reasonable conclusions.

Keywords: Experiment, Analysis, Distortion, Welding, Stiffened plates

1 INTRODUCTION

The global and local behavior of plated-marine structures normally depends on multiple variables some of them are related to construction material (mechanical properties), geometrical configurations, boundary conditions and others concerning loading and operational conditions.

Plates are considered as the main structural components of marine structures, and the geometrical configuration of such plating is essential to withstand different acting loads, in addition to the stiffening members. These plates are subjected to combined loads, axial loads (tension or compression), shear loads, and lateral loads mainly due to water pressure. The existence of the plates in both perfect or imperfect condition and especially imperfect with different imperfection rates will dominate the structural response.

The main cause of plate imperfections is the welding process which is used to join two plates together or to attach a stiffening member. The consequences of welding are post-weld initial imperfection and residual stresses.

Masubuchi [1] concluded that the plate welding induced distortions may be categorized into six patterns: transverse shrinkage, angular, rotational distortion, longitudinal shrinkage, buckling, and longitudinal bending, as illustrated in Figure 1; this generally affects the buckling strength of the plates. The induced residual stresses may be idealized in to a pattern based on experiment as the one given by Faulkner [2] and presented in Figure 2. It was reported that the value of η (tension block) are typically 4.5 to 6 for as-welded ships, but values of 3 to 4.5 are more appropriate for ship design after allowing for shake-out at sea, Faulkner [2].

To ensure equilibrium along the direction of the attached stiffener, both tension and residual compression

blocks must be balanced, considering that the compression exists largely in the plate. This balance may be expressed as given in Eq. (1), where σ_{rc} is the residual compressive stress, σ_y is the material yield stress, b is the width between stiffeners and t_p is the plating thickness. This equation is valid for plate slenderness β >1,and it was reported by Faulkner [2] that the peak value of the residual compressive stress may reach 0.75 σ_y according to the fabricated test sections; however, for ship structures, the value is generally around 0.25σ_y.

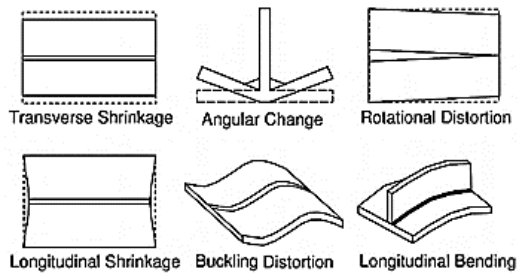

Figure 1: Patterns of welding distortion, Masubuchi [1]

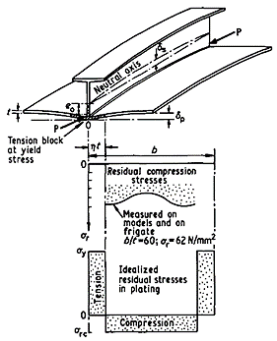

Figure 2: Idealized residual stress pattern, Faulkner [2]

$$\frac{\sigma_{rc}}{\sigma_y} = \frac{2\eta t_p}{b - 2\eta t_p} \quad (1)$$

Lightfoot et al. [3] applied the artificial neural networks for studying the weld- induced distortion considering multiple variables as thickness, steel grades, and preparation process and heat source input. It was found that the most significant variable to the distortion is the heat input followed by carbon contents in the base plate.

Numerically, Gannon et al. [4] studied the effect of fillet welding sequence on both induced residual stresses distribution and initial distortion for stiffened steel plates. Based on the performed analysis, a welding sequence pattern was proposed which resulted in lower residual stresses and distortion. Both initial and post-collapse distortion are analysed by Saad-Eldeen et al. [5] for 36 plates between stiffeners of three box girders. A slenderness criterion was developed to predict the collapse shape based on initial imperfection.

Chen and Guedes Soares [6] reported the distortion results from butt welding for plates measured using 3D measurement technique with the aid of close-range photogrammetry.

Experimental and numerical prediction of weld induced imperfection are performed by Chen and Guedes Soares [7] for square steel plates to account for its effect on the compressive strength capacity. It was reported that as the plate slenderness decreases from 3.8 to 1.6, the weld induced displacement decreases due to increasing the plate thickness.

Experimentally four large stiffened panels are tested by Podder et al. [8] considering different welding sequences and an appropriate sequence is suggested for minimum weld-induced distortions. Thermal elasto-plastic finite element comparative analysis are performed by Chen et al. [9] for welding procedures of stiffened panels. It was concluded that both residual stresses and welding distortion are sensitive to the welding procedure for the same heat input.

Experimental analyses are presented in Urbański et al. [10] for the distortion of fixed butt-welded plates using a design of experiment (DoE) approach, and it was stated that the approach and the results may be applied for large scale structure.

Cao et al. [11] analysed the welding distortion of thick plates considering the effect of welding sequence and flam heating on distortion mitigation. It was reported that around 20% reduction in the plate distortion may arise with the application of flam heating.

Cao et al. [12] predicted the distortion of ship plate-frame structure numerically using a self-learning database. It was reported that a reasonable welding sequence may reduce the distortion of the structure by 11.2%.

Wahidi et al. [13] presented a comprehensive review on the applications of robotic welding in the marine sector, in addition to the human-robot collaboration for enhancing productivity and ensure workers safety.

The motivation of the present research work is to distinguish the effect of different welding geometries; continuous and intermittent chain fillet welding on the transverse weld-induced imperfections for square stiffened steel plates accounting for different plating thickness. Also, to compare the test results by existing empirical formations, which may enhance the decision making for selecting the appropriate weld geometry for specified locations.

2 Preparations and Testing of the Specimens

Mild steel stiffened plate specimens are prepared and welded in Port Said shipyard owned by Suez Canal Authority; they are attached together using shielded metal arc welding. After welding, the induced initial imperfections are measured, and a nondestructive test is applied to ensure the welding quality.

2.1 Specimens Geometrical Configurations

The welded specimens are square steel plates with length and breadth *L*, *B* of 500 mm, respectively, with one attached flat bar stiffener of height h_w and thickness t_w of 80 and 10 mm, respectively, see Figure 3. The geometrical description of both plate and stiffener used in the present analysis are given in Table 1, where variant plating thicknesses are used as 6 mm, 8 mm, and 10 mm, with constant stiffener configurations. The chemical compositions of the used shipbuilding steel plates are given in Table 2, with yield strength, tensile strength, and elongation of 341 MPa, 487 MPa and 39%, with gauge length $5.65\sqrt{S_0}$, where S_0 is the original cross-sectional area of the tensile test specimen, as specified in the material certificate.

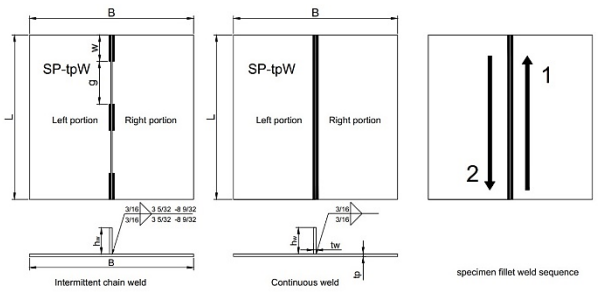

(a) (b) (c)

Figure 3: Cross-sectional details of the welded stiffened plate, (a) intermittent chain, (b) continuous and (c) welding sequence

Table 1. Geometrical configurations of the welded specimens, mm

SP-ID	L	B	t_p	h_w	t_w
SP-6C	500	500	6	80	10
SP-8C			8		
SP-10C			10		
SP-6I			6		
SP-8I			8		
SP-10I			10		

Table 2. Material Chemical composition

	C $x10^{-2}$	Si $x10^{-2}$	Mn $x10^{-2}$	P $x10^{-3}$	S $x10^{-3}$	Al $x10^{-3}$
Min.						**20**
Max.	**21**	**50**		**35**	**35**	
	17	16	97	12	5	21

Two types of fillet welding are applied to attach the stiffener; continuous (C) and intermittent chain welding (I), reveals to specimen ID defined as follow (SP-t_pW), where SP is the stiffened plate, t_p is the plating thickness and W is the welding type. Therefore, SP-6C refers to the stiffened plate of 6 mm plating thickness and the stiffener is attached using continuous fillet welding as defined Table 1.

The welding of the flat bar stiffener is carried out by manual metal arc welding with current, voltage and speed of 180-200 Ampere, 40-50 Volt and 2.4-2.6 mm/sec. The welding electrode is E6013 with 4mm diameter, which is used for welding mild steel in shipbuilding applications and approved by LR's Grade 2Y.

The applied and approved welding geometry is presented in Figure 3, where for intermittent chain welding the weld length (w) = 80mm and the weld gap (g)=130mm. For each specimen, the attachment of the stiffener is carried out using two welding passes, starting from the right portion of the plate, where the fillet weld sequence is shown in Figure 3 (c). During the welding process, the four edges of the square plate are not constrained, imposing free boundary conditions.

A sample of the welded specimens using two welding configurations is presented in Figure 4 for continuous (left) and intermittent chain fillet welding (right).

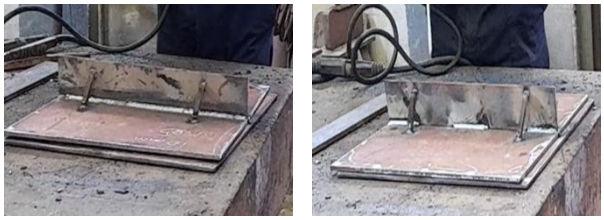

Figure 4: Sample of welded specimen using with continuous (left) and intermittent chain (right) fillet welding

2.2 Non-destructive Test

After performing the welding process for all specimens, each specimen is tested separately using magnetic particles nondestructive test by a certified quality control engineer belongs to Port Said shipyard, to ensure the welding quality, where a sample of the magnetic particles examination report is presented in Figure 5. The report confirmed that the welding procedure was performed without any induced cracks.

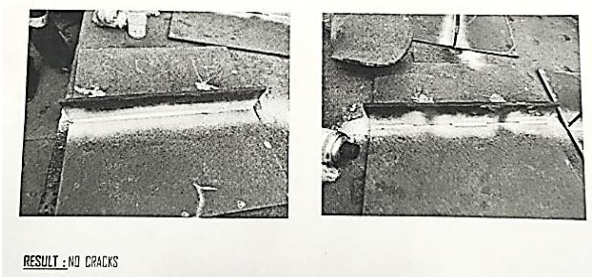

Figure 5: Sample of magnetic particles examination test for welded specimens with continuous (left) and intermittent chain (right) fillet welding

3 Imperfection Measurements and Analysis

Due to welding, initial distortion or imperfection may occur, and depending on the number and sequence of welding passes as well as the base plating thickness, the imperfection amplitude may vary.

3.1 Induced Initial Imperfection for Specimens with Continuous Fillet Welding (C)

Before performing the welding experiment, both base plating and stiffener are almost flat. During welding process, two parameters were observed: welding time for both first and second pass and number of consumed electrodes. For each specimen, the measurements of the initial imperfections are recorded at the two extreme edges along the plate width B/2 as -250 mm for left portion and 250 mm for the right portion), where zero is the location of the stiffener.

For specimen SP-6C, the estimated time for the first pass was 284 seconds, where for the second pass the time decreases to 265 seconds, with a total number of consumed electrodes of 4.5. After the first pass (right portion), see Figure 3, the plate distorted upward with measured initial distortion in the right and left portions of 5.5 mm and 3.5 mm, respectively (see Figure 6). After applying the second welding pass (left portion), the initial distortion amplitude changed to 6 mm and 13 mm, in the right and left portion, respectively, as presented in Figure 6.

Figure 6: Measured initial imperfection due to welding along the plate width, SP-6C

Table 3. Measured initial imperfection amplitude (mm), for continuous (C) welded specimens

SP-ID	Pass sequence	Left portion	Middle	Right portion
SP-6C	1st	+3.5	0	+5.5
	2nd	+13	0	+6
	Relief	+8	0	+5
SP-8C	1st	+6	0	+2
	2nd	+4.5	0	+4
	Relief	+6	0	+6
SP-10C	1st	0	0	+1.5
	2nd	+2.5	0	+6.5
	Relief	+5	0	+6

As a result of heat relief (the specimen becomes cold), the initial distortion was measured, showing lower imperfection amplitudes than the ones measured immediately after the second pass, with final amplitudes of 5 mm and 8 mm, in the right and left portion, respectively. Based on the measured distortion amplitude, it is obvious that distortion is asymmetric (upward) with higher amplitude in the left portion, as tabulated in Table 3 and presented in Figure 6 by dot lines.

As the base plating thickness increases to 8 mm, specimen SP-8C, with the same attached stiffener used in the previous test, the first pass took 259 seconds, while the time of the second pass was 250 seconds, which is less than the elapsed time for specimen SP-6C. On contrary, the number of consumed electrodes for SP-8C is 4.75 electrodes, which is higher than the one for SP-6C (4.5 electrodes). Regarding the measured initial imperfections, the first pass results in upward imperfection in the right and left portion of 2 mm and 6 mm, respectively, see Figure 7. By the application of the second pass, the right and left imperfection reached 4 mm and 4.5 mm, respectively. After heat relief, the specimen recorded final upward symmetric initial imperfection of 6 mm as given in Table 3 and presented in Figure 7.

For thicker plating of 10 mm, SP-10C, the required time for finishing the first and second pass is 252 second and 257 second, respectively, while five electrodes were consumed. The resultant imperfection due to the first pass is 1.5 mm and zero at the right and left portion, respectively, see Figure 8. As the second pass started, the imperfection at both right and left portion increases until reaching 6.5 mm and 2.5 mm, respectively. After reaching the ambient temperature (heat relief), the registered imperfection at the right portion decreases to 6 mm and the left portion increases to 5 mm, resulting in less asymmetric shape, as presented in Table 3 and Figure 8.

Based on the performed analysis for the three different base plating thicknesses with constant attached flat bar stiffening geometrical configurations and used continuous fillet welding, it was observed that the induced imperfection at the location of the second pass decreases as the plating thickness increases.

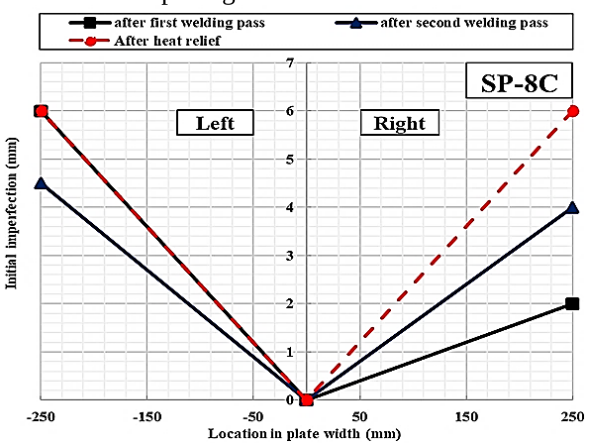

Figure 7: Measured initial imperfection due to welding along the plate width, SP-8C

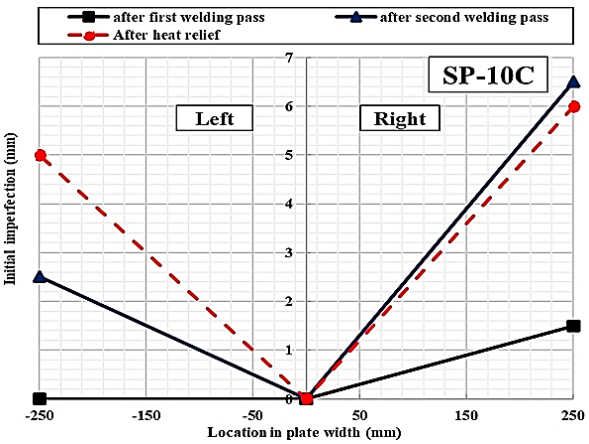

Figure 8: Measured initial imperfection due to welding along the plate width, SP-10C

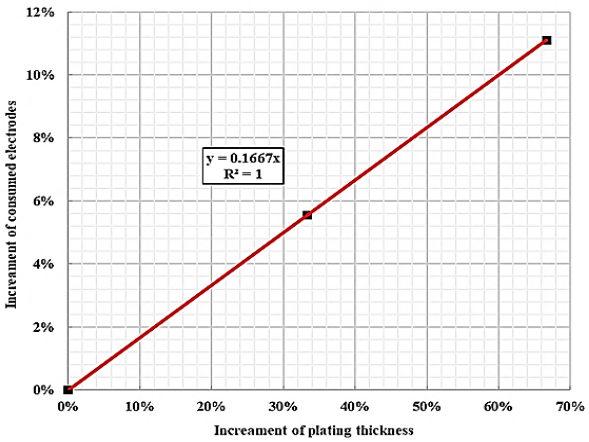

Figure 9: Relationship between increment of plating thickness and consumed electrodes for continuous weld specimens

Also, the global induced initial imperfection amplitude decreases as the plating thickness increases, which agrees with the work done by Chen and Guedes Soares [7]. Additionally, as the plating thickness increases, the resultant imperfection shape and amplitude is almost symmetric. The effect of preheat temperature due to the 1st pass decreases as the plate thickness increases, which is represented by lower imperfection amplitude after the 2nd pass.

Furthermore, as the base plating becomes thicker, the consumed number of electrodes increases linearly, and the increment percentage may be fitted to regression equation as shown in Figure 9.

3.2 Induced Initial Imperfection for Specimens with Intermittent Chain Fillet Welding (I)

For such welding experiment, the welding process is performed using intermittent chain welding considering the welding geometry presented in Figure 3.

Three specimens of different base plating thickness are studied as the same of continuous welding. The first one with plating thickness 6 mm, SP-6I, the time required for performing the first pass was 138 second, while the second pass takes 135 second, with total consumption of 2.5 electrodes. It was observed that the induced initial imperfections due to the first welding pass are 6 mm and 1 mm in the right and left portion respectively, as given in Table 4 and presented in Figure 10 .

After the application of the second pass, the imperfection amplitude in both right and left portions increase to 9 mm and 3 mm, respectively. Leaving the specimen until reaching the ambient temperature and the induced heat is relieved; the final induced imperfection shape is asymmetric with 9 mm and 2 mm, at the right and left portion, respectively.

As the plating thickness increases to 8mm, SP-8I, the required time for completing the first and second passes is the same of 133 second, keeping the same amount of 2.5 electrodes. The initial induced imperfections due to the first pass in both right and left portion are 1 mm and 1.5 mm, respectively. Due to the second pass, both imperfection amplitudes increase to 1.5 mm and 2 mm, respectively. After heat relief, the specimen showed asymmetric amplitude of 4 mm right and 2 mm left, see Figure 11 and Table 4, which is less than the inducted imperfection for SP-6I.

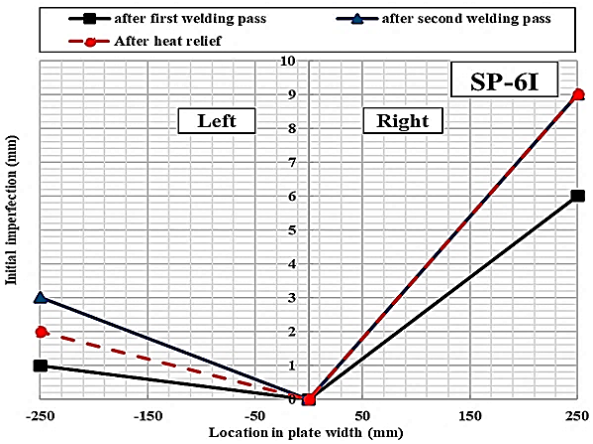

Figure 10: Measured initial imperfection due to welding along the plate width, SP-6I

Table 4. Measured initial imperfection amplitude (mm), for intermittent chain (I) welded specimens

SP-ID	Pass sequence	Left portion	Middle	Right portion
SP-6I	1st	+1	0	+6
	2nd	+3	0	+9
	Relief	+2	0	+9
SP-8I	1st	+1.5	0	+1
	2nd	+2	0	+1.5
	Relief	+2	0	+4
SP-10I	1st	Zero	0	+1.5
	2nd	+1.5	0	+2.5
	Relief	+1.5	0	+2

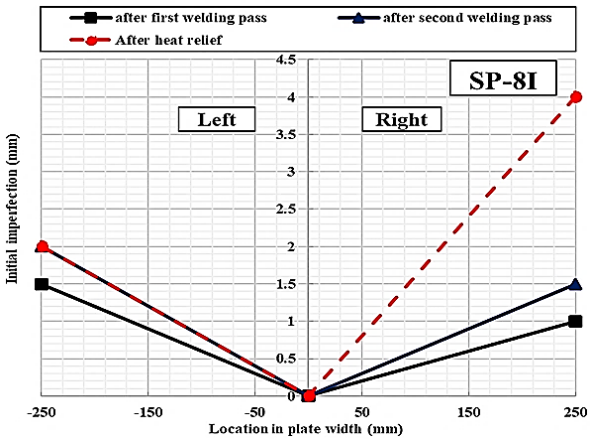

Figure 11: Measured initial imperfection due to welding along the plate width, SP-8I

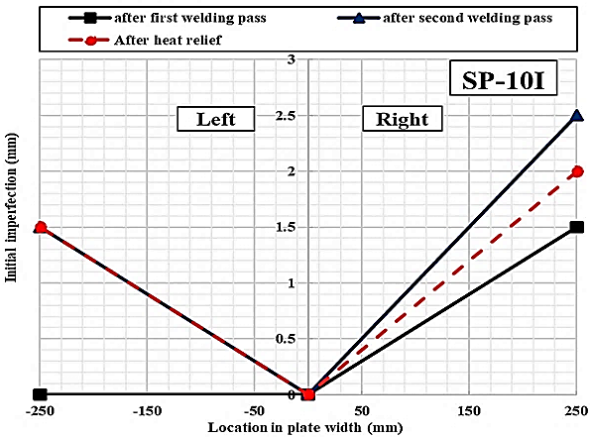

Figure 12: Measured initial imperfection due to welding along the plate width, SP-10I

For thicker plating, t_p 10 mm, SP-10I, the required time for carrying out the welding passes is 129 second and 141 second, respectively, with the same electrode consumption of SP-6I and SP-8I. After the first pass, the measured initial imperfection amplitudes are 1.5 mm and zero, for the right and left portion, which increases to 2.5 mm and 1.5 mm after the application of the second pass.

The final imperfection amplitude after heat relief reaches 2 mm right and 1.5 mm left; see Figure 12 and Table 4, which are less than the registered amplitudes for both SP-6I and SP-8I.

Therefore, it may be stated that for intermittent chain welding experiment using three different plating thickness of 6 mm, 8 mm and 10 mm, the induced initial imperfection at the left portion (location of the 2nd pass) decreases as the plating thickness increases, which agrees with the one of continuous welding. Also, as the plating thickness increases, the final induced initial imperfection amplitude decreases which also in agreement with specimens of continuous welding. On contrary to continuous welding, the plating thickness has no effect on the consumed electrodes (constant consumption 2.5 electrodes). Also, the final induced imperfection due to intermittent chain welding is lower than that induced by continuous welding and the amplitude decreases as the plating thickness increases.

4 Comparative Analysis

A relationship between the welding time for each welding type (continuous and intermittent chain) and base plating thickness for the three specimens is presented in Figure 13. It is obvious that the C-welding time is higher than that for I-welding and both relationships may be fitted to nonlinear function.

The ratio between continuous and intermittent chain welding time as a function of plating thickness is presented in Figure 14. The trend is nonlinear and may be fitted with polynomial function, showing that the ratio decreases as the plating thickness increases.

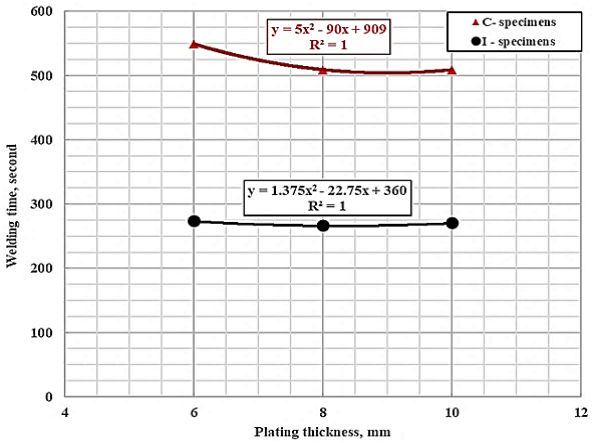

Figure 13: Relationship between plating thickness and welding time

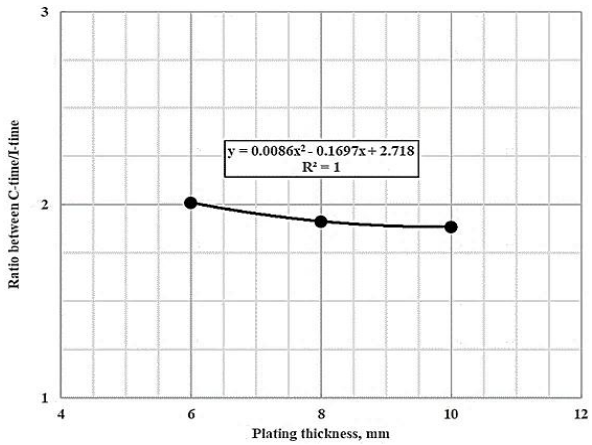

Figure 14: Relationship between plating thickness and ratio of welding time C/I

One of the main controlling parameters in buckling analysis for steel plated structure is the plate slenderness β which is defined as a function of plate geometry; breadth between stiffeners b, plating thickness t_p and

material mechanical properties; yield stress σ_y and modulus of elasticity E, as given in Eq. (2).

$$\beta = \frac{b}{t_p}\sqrt{\frac{\sigma_y}{E}} \tag{2}$$

According to the material certificate of the used normal shipbuilding steel provided by the shipyard, both material properties σ_y and E, are 341 MPa and 206 GPa, respectively, which reveals that the plate slenderness of the tested specimens is 2.03, 2.54 and 3.39, respectively. The relationship between plate slenderness and average welding induced imperfection amplitude for specimens with different welding types is shown in Figure 15. The experimental results may be fitted with power function and the deviation between the average induced imperfection amplitude decreases as the plate slenderness increases.

A comparison between the measured induced initial imperfection amplitudes for the free ends welded stiffened plates and existing empirical expressions by Faulkner [2] and Smith et al. [14], Eq.(3) and Eq.(4), respectively, for simply supported stiffened plates is presented in Figure 16.

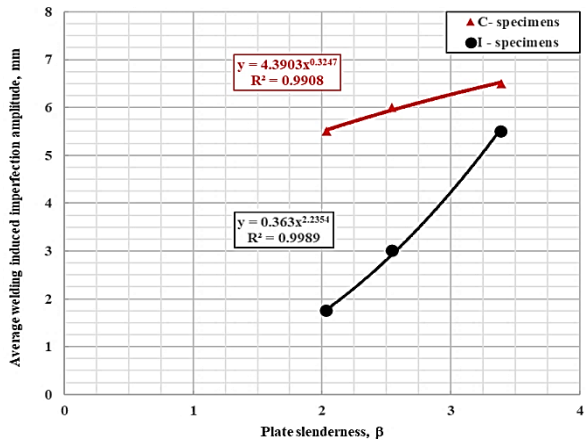

Figure 15: Relationship between plate slenderness and average welding induced imperfection amplitude for different welding configurations

$$\frac{\delta_p}{t_p} = 0.12\beta^2\left(\frac{t_w}{t_p}\right) \tag{3}$$

$$\frac{\omega_{opl}}{t_p} = \begin{cases} 0.025\beta^2 & for\ slight\ level \\ 0.1\beta^2 & for\ average\ level \\ 0.3\beta^2 & for\ serious\ level \end{cases} \tag{4}$$

where t_w is the stiffener thickness, δ_p and ω_{opl} are the imperfection amplitude. It is obvious that the measured amplitudes for continuous welding presented in Figure 16 (a) are within range with respect to the estimated ones by both equations with some overlap. The reason could be attributed to the type of boundary conditions (free for tested specimens and simply supported for empirical ones). For intermittent chain welding, Figure 16 (b), the measured imperfection amplitudes are also lower than the calculated ones by Faulkner [2] and Smith, Davidson et al. [14], such behavior might be due to the smaller amount of welding used to attach the stiffener, and the lower induced thermal stresses, keeping the boundary conditions free.

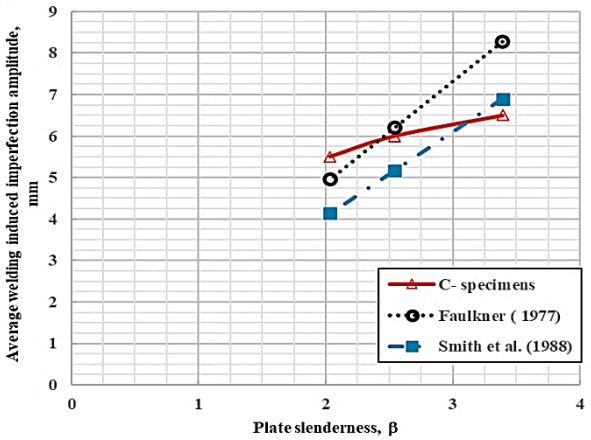

(a)

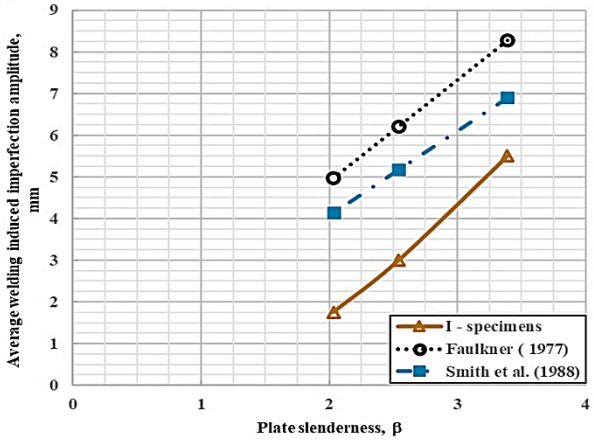

(b)

Figure 16: Comparison between experimental results for free C&I welded specimens and empirical formulation for simply supported plates

5 CONCLUSION

A series of experimental welding tests are performed for a square stiffened plate with different base plating thickness, the stiffener is attached using two different fillet welding geometries: continuous and intermittent chain. The induced initial imperfections are measured and analyzed. Based on the performed analysis the following conclusions are stated:

- For continuous fillet welding, the global induced initial imperfection amplitude decreases as the plating thickness increases. The effect of preheating temperature due to the 1st pass decreases as the plate thickness increases, which is represented by lower

imperfection amplitude after the 2nd. As the base plating becomes thicker, the consumed number of electrodes increases linearly.

- For intermittent chain welding, a good agreement with the continuous welding regarding the decrease of imperfection amplitude as the plating thickness increases, but with higher rate for intermittent welding. On contrary to continuous welding, the plating thickness has no effect on the consumed electrodes.
- The trend of the ratio between continuous and intermittent chain welding time as a function of plating thickness is nonlinear and the ratio decreases as the plating thickness increases.
- A comparison between existing empirical formulations and the experimental results is performed, showing reasonable results.

Credit Authorship Contribution Statement

S. Saad-Eldeen: Concept, Methodology, Original draft, Review and Editing, Supervision

M-Allah Eltaramsy: Concept, Methodology, Original draft

M. Mansour: Concept, Review and Editing, Supervision

Declaration of competing Interest

The authors declare that they have no known competing financial interests or personal relationships that could have appeared to influence the work reported in this paper.

Declaration of Funding

This research received no external funding.

6 REFERENCES

1. Masubuchi, K., Analysis of welded structures - residual stresses, distortion, and their consequences1980: Pergamon Press, Oxford.
2. Faulkner, D., Effects of Residual Stresses on the Ductile Strength of Plane Welded Grillages and of Ring Stiffened Cylinders. The Journal of Strain Analysis for Engineering Design, 1977. 12(2): p. 130-139.
3. Lightfoot, M.P., et al., Artificial neural networks – an aid to welding induced ship plate distortion? Science and Technology of Welding and Joining, 2005. 10(2): p. 187-189.
4. Gannon, L., et al., Effect of welding sequence on residual stress and distortion in flat-bar stiffened plates. Marine Structures, 2010. 23(3): p. 385-404.
5. Saad-Eldeen, S., Y. Garbatov, and C. Guedes Soares, Analysis of Plate Deflections during Ultimate Strength Experiments of Corroded Box Girders. Thin-Walled Structures, 2012. 54: p. 164-176.
6. Chen, B. and C. Guedes Soares, Deformation measurements in welded plates based on close-range photogrammetry. Proceedings of the Institution of Mechanical Engineers, Part B: Journal of Engineering Manufacture, 2016. 230(4): p. 662–674.
7. Chen, B. and C. Guedes Soares, Effects of plate configurations on the weld induced deformations and strength of fillet-welded plates. Marine Structures, 2016. 50: p. 243-259.
8. Podder, D., S. Das, and N.R. Mandal, Distortions in Large Stiffened Ship Panels Caused by Welding: An Experimental Study. journal of Ship Production and Design, 2019. 35(3): p. 250–262.
9. Chen, Z., et al., Comparative study of welding deformation of a stiffened panel under various welding procedures. Proceedings of the Institution of Mechanical Engineers, Part B: Journal of Engineering Manufacture, 2019. 233(1): p. 182-191.
10. Urbański, T., A. Banaszek, and W. Jurczak, Prediction of welding-induced distortion of fixed plate edge using design of experiment approach. Polish Maritime Research, 2020. 27(1): p. 134-142.
11. Cao, Y., et al., Welding distortion prediction and mitigation in thick steel plate structures on ships. Ships and Offshore Structures, 2022. 17(12): p. 2674-2685.
12. Cao, Y., et al., Welding distortion prediction of ship plate frame structures based on a self-learningdatabase. Ships and Offshore Structures, 2023. 18(11): p. 1606-1616.
13. Wahidi, S.I., S. Oterkus, and E. Oterkus, Robotic welding techniques in marine structures and production processes: A systematic literature review. Marine Structures, 2024. 95: p. 103608.
14. Smith, C.S., et al., Strength and Stiffness of Ships' Plating under In-plane Compression and Tension. Transactions RINA, 1988. 130: p. 277-296.